

**Research Article**

## **OBTAINING THE CURVES OF COMPRESSIVE FLOW STRESS OF AZ60 MAGNESIUM ALLOY**

**\*Mohammad Loveymi, Abaas Talimiyan and Farzan Barati**

*Department of Mechanics, Science and Research Branch, Islamic Azad University, Hamedan, Iran*

*\*Author for Correspondence*

### **ABSTRACT**

In this paper, obtaining the curves of pressure flow stress of magnesium alloy AZ60 has been considered. Today the magnesium alloys due to their properties are used in industries such as aerospace, car manufacturing, and electronics and their applications are increasing. In this experiment, the pressure tests on magnesium alloy AZ60 are conducted at room temperature and with different speeds between 0.5 to 5 mm per minute over the cylindrical specimens. Experiments have been done by a device called SANTAM 150KN. The initial amount of stress was calculated with convexity correction factor and then by Deform-2D software and multi-stage correction values of numerical stress-strain was obtained for the alloy. The results show that, with increasing strain, stress rate increases until reaches to the maximum point, and in fact, this material has the behavior of hardness. Also at room temperature, with increasing loading rate of compressor, the stress-strain curve does not change much.

**Keywords:** *Magnesium Alloys, Compression Test, Correction Factor, Friction, Temperature, Strain Rate*

### **INTRODUCTION**

Today, light alloys are very widely used in industry. One of these groups of alloys is magnesium. Due to the high melting temperature and very good resistance of this element and its alloys against corrosion, the alloys of this element are broadly used in aerospace industry and industry of manufacturing ornaments. Also some of magnesium alloys have a good compatibility with the human body that this property has caused to be used in making implant. Due to the importance of using magnesium alloys, stress-strain behavior of this alloy is very important and considerable. Since these alloys are formed in the elevated temperatures, the behavior of flow curves is very important. Each of elevated temperature tests has very high cost; therefore, if we can model the behaviors of these alloys, we can save the time and the cost. Sheng and Shivpuri (2006) performed the modeling of flow stress of magnesium alloys at elevated temperatures. Therefore, the analysis of deformation mechanisms of magnesium alloy at high temperatures and different strain rates, an analytical model is proposed to describe the development of the flow stress. Zener-Halloman parameter that represents the combined effects of temperature and strain rate is introduced. The model was approved on three experimental data. The comparison shows that the stress of predicted flow by the model is in good agreement with the measured experimental values. Wang *et al.*, (2007) studied the characteristics of hot deformation of compression casting alloy of ZK60 using process maps. The results show that the flow stress decreases with decreasing strain rate and increasing deformation temperature. Chang *et al.*, (2008) conducted research on the microstructure and mechanical properties of AZ31 magnesium alloy plate made by asymmetric hot extrusion at temperature of 673°K. The results show that the grain size of AZ31 magnesium alloy plate with different rolling rate at high temperatures can be decreased up to 3 $\mu$ m. Extruded sample AZ31 asymmetrically showed a fine grain microstructure and some gradients of grain size and heterogeneous distribution of texture across the thickness. Yang *et al.*, (2008) investigated hot compression behaviors of Ti-6Al-2Zr-1Mo-1V alloy at temperature of 1073°K and evaluation of the microstructure during deformation process. The results show that the flow stress increases upward to reach a peak stress, then disappears with increasing strain and finally the Figures reach a steady state. Yakin *et al.*, (2008) performed the analysis of the stress flow on D and ZK60 magnesium alloys during deformation at high temperatures. Results show that the thermal simulated curves of different alloys in the same deformation conditions vary. General curves of AZ31 and AZ91 D alloys have dynamic re-crystallization properties. Maghsoud *et al.*, (2009) carried out a research

### Research Article

on the effect of strain rate and temperature on the deformation capability and development of the microstructure of AZ31 magnesium alloy using mechanical tests such as hardness and tensile tests. Further investigation was performed to connect the behavior of matter with development of the microstructure through studying the volume fraction and dynamic re-crystallization grain size. The results show that at high temperatures and low strain rate, the peak of stress decreases while the volume fraction and dynamic re-crystallization grain size increase. This phenomenon can be attributed to the dynamic re-crystallization process. Shaming *et al.*, (2009) performed mathematical modeling of flow behavior at high temperatures for Ti-45Al-8.5Nb-(W, B, Y) alloy. A mathematical model has been created for predicting the stress-strain curves in the base alloy TiAl included high Nb during hot deformation. This model is based on a representation of the stress-strain curves, which can be shown by Zenir-Hollman parameter at a hyperbolic sine function.

Liang *et al.*, (2009) investigated the corrosion behavior of four types of the rolled magnesium alloys AZ91, AM60, ZK60, and AZ31 in 1mol /L sodium chloride solution. The results show that the corrosion resistance of four matters is ZK60> AZ91> AM60> AZ31 respectively. Wang *et al.*, (2009) studied the rate of sensitivity to strain rate of magnesium casted alloys. They evaluated the behaviors of three alloys AM20, AM50 and AM60 on a wide range of strain rate, from strain rate of  $0.001\text{ s}^{-1}$  to  $1700\text{ s}^{-1}$ . The results show that at low strain rates, the sensitivity rate to strain rate decreases by increasing the amount of aluminum alloy in magnesium alloy. Yang *et al.*, (2009) carried out a research on the flow stress of AZ31 and ZK60 magnesium alloys using hot compression deformation tests at different temperatures and strain rates. The results show that the thermal simulation curves of AZ31 and ZK60 have different shapes under identical deformation conditions. The curves of AZ31 have the characteristics of dynamic re-crystallization and the flow stress increases to a peak value, and then decreases to a steady state. Renlong *et al.*, (2009) studied the behavior of dynamic re-crystallization of magnesium alloy under pressure and they were able to predict the behavior of the alloy. The results show that the strong basic texture after 50% of pressure ( $\varepsilon = 0.69$ ) can be seen on samples of hot and extruded rolls that have different primary textures. Jiang Qin *et al.*, (2010) carried out the flow stress modeling for magnesium alloy during hot deformation. Hot compression tests were conducted to investigate the flow behavior of ZK60 magnesium alloy. This model is able to predict the behavior of work hardening and dynamic recovery zone and also softening resulting from dynamic re-crystallization. Kim *et al.*, (2010) carried out a research on the development of ultra-fine grain microstructure of magnesium alloy plates. Mg-3Al-1Zn alloy was produced with completely re-crystallized microstructure with an average grain size of  $1\mu\text{m}$  with rolling and under the chosen high speed rates under cold plate conditions subjected to hot rolling, and hence the total thickness is decreased by 68% after two times of rolling. Lee *et al.*, (2010) estimated and obtained the flow behavior and alloy processing map of Mg-10Gd-4 /8Y-2Zn-0/6Zr. The tests pressure of this alloy were performed in the temperature range from  $350^{\circ}\text{C}$  to  $500^{\circ}\text{C}$  and the strain rate range from  $0.001\text{ s}^{-1}$  to  $\text{s}^{-1}$ .

Yan *et al.*, (2010) investigated hot deformation behavior and microstructure development of ZK21 magnesium alloy in the temperature range  $250\text{--}400^{\circ}\text{C}$  and strain rate range  $(0.1\text{--}50)\text{ s}^{-1}$ . At temperatures above  $350\text{--}400^{\circ}\text{C}$  and strain rate lower than ( $\leq 1\text{ s}^{-1}$ ), dynamic re-crystallization occurs and develops mainly at the grain boundaries. Yun-Bin *et al.*, (2010) carried out a research on the effect of two-step pressing in identical angular channels on the microstructure and mechanical properties of the extruded ZK60 alloy. The results show that fine grain size less than  $1\mu\text{m}$  after a two-step process of ECAP, 4 passes on 513K, and then 4 another passes in 453K is obtained. Anbuselvan and Ramanathan (2010) studied deformation of ZE41A magnesium alloy using a compression test. Temperature range of their compression tests has been  $300\text{ to }500^{\circ}\text{C}$ . Their research showed that the temperature and strain rate are important in shaping the magnesium alloy. Also, the optimal parameters in forming ZE41A magnesium alloy are the temperature of  $400^{\circ}\text{C}$  and strain rate of  $0.001\text{ s}^{-1}$ . Fu-Sheng *et al.*, (2010) investigated the effects of impurities on the microstructure and mechanical properties of ZK60 magnesium alloys by optical microscope, electronic microscope, and tensile test. The results show that the yield strength of ZK 60-45 alloys with low impurity increases up to 295Mpa after T5 operation. Chen *et al.*, (2011)

### Research Article

investigated hardening strain behaviors of extruded alloy of magnesium under various heat treatments (T4, T5 and T6) using uniaxial tensile tests at room temperature.

In T5 and T6 treatments, the strain hardening of extruded ZK60 alloy reduces, and after increasing it reaches to an apparent reduction in tensile uniform strain. Shin *et al.*, (2011) carried out a research on the microstructure refinement and improvement of ZK60 magnesium alloy properties with hotrolling.

Tensile tests show that the yield strength with starting of 202MPa and ultimate strength of 307MPa in rolling and transverse direction of finished plates are identical.

Yan *et al.*, (2011) examined the effect of aging on microstructure and mechanical properties of AZ80 and ZK60 magnesium alloys by optical microscope and mechanical testing machine. The results show that the tensile strength and the increase in the length of AZ80 alloy, when the aging temperature increases, initially increase and then decrease. Legerski *et al.*, (2011) conducted a research on the model of static re-crystallization of AZ31magnesium alloy. The used metallographic methods showed that the re-crystallization process in the studied materials occurs at temperature of 523°K and higher.

Chen *et al.*, (2012) carried out a research on the development of the microstructure, mechanical properties, and formability of Mg-Zn-Y-Zrmagnesium alloy that are subjected to direct extrusion in different conditions.

The results show that the mechanical properties of this alloy, when the extrusion temperature increases from 400 to 450°C, become considerably worse. Bin *et al.*, (2012) performed modeling of strain hardening and dynamic re-crystallization of ZK60 magnesium alloy during hot deformation.

The results show that the softening effect mainly occurs due to dynamic recovery in initial strain hardening phase and changes of dynamic re-crystallization after the stress reaches a peak value. Changizian *et al.*, (2012) carried out the modeling of the high temperature flow behavior of AZ81 magnesium alloy with considering the effects of strain through doing hot compression tests in the temperature ranges of 250-450°C and at different strain rates (0.3, 0.03, 0.003) s<sup>-1</sup>. The results confirmed the predictability of the developed model. Barati *et al.*, (2012) performed the modeling of the behavior of AZ group magnesium alloys in stress and pressure using mathematical material model at high temperatures and different strain rates.

Deformed microstructures of AZ80 show that the lower the temperature or strain rate, the greater the average grain size in the sample. Lee and Dong (2013) studied the effect of solution heat treatments on the microstructure and hardness of ZK60 magnesium alloy.

The results show that comparing with the microstructure observed in the absence of an electromagnetic field, the eutectic network structure at grain boundaries is better found under low frequency alternating magnetic field and is displayed as uniform grain distribution.

In the present study, obtaining the curves of compressive stress flow of AZ60 magnesium alloy is studied. As seen in previous studies, obtaining the curves of compressive flow stress for alloy magnesium is not observed. In this regard, some models have been provided to study the behavior of AZ60 magnesium alloys in different strain rates at room temperature.

### The Basic Equations and Tests Used

#### Compression Test

In this experiment, some compressors with flat plates compress a cylindrical specimen. In an ideal state and under conditions of zero friction, during compaction of cylinder specimen, the barreled state does not occur and the specimen remains cylindrical (Figure 1). However, frictional ways exists and creation of these ideal conditions is impossible, therefore, the specimen always deforms in the form of a barrel (Saniei and Fatehi, 2006).

**Research Article**

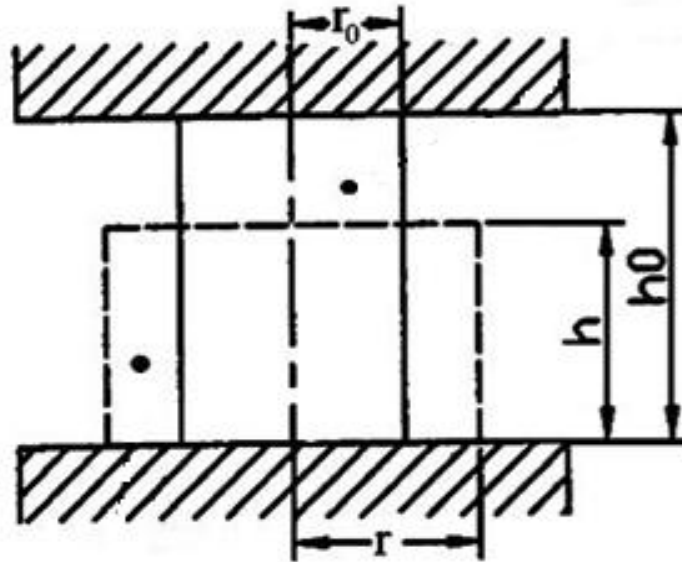


**Figure 1: Schematic view of compression test under conditions of zero friction**

At each stage, the change in diameter of each sample is recorded. The following equations are valid for uniform compression test.

$$\bar{\epsilon} = \ln \frac{h_0}{h} = \ln \frac{A}{A_0} \quad (1)$$

$$\bar{\sigma} = \frac{P}{A} \quad (2)$$

Where,  $A_0$  and  $A$  are the moment and initial section areas,  $h$  and  $h_0$  are the moment and initial heights and  $\bar{\epsilon}$  and  $\bar{\sigma}$  are effective strain and effective stress respectively and  $P$  is the force exerted on the specimen.

*The Method of Convexity Correction Factor*

Since, the barrel state of samples is inevitable, so a method is used which is called convexity correction factor to correct the error resulting from the multi-axial stress due to creation of barrel state in the specimen. In the method of convexity correction factor, material flow stress is determined using stress analysis of middle section of a pressurized cylindrical sample between two parallel plates. In this analysis, it is assumed that the materials are homogeneous, isotropic, and incompressible. Considering the equilibrium condition in the radial direction  $r$  which is shown in Figure 2, and using geometrical conditions and plasticity equations, the following equations are obtained using mathematical calculations (Milnick, 1981):

$$\sigma_r = \bar{\sigma} \ln\left(\frac{a^2 - 2aR - r^2}{-2aR}\right) = -\bar{\sigma} \ln\left(\frac{2aR}{2aR - a^2 + r^2}\right) \quad (3)$$

$$\sigma_z = \bar{\sigma} \left[1 + \ln\left(\frac{a^2 - 2aR - r^2}{-2aR}\right)\right] = \bar{\sigma} \left[1 + \ln\left(\frac{2aR}{2aR - a^2 + r^2}\right)\right] \quad (4)$$

Where,  $\bar{\sigma}$  is the effective stress of the material, and in Von Mayors criterion, it is calculated from following equation:

$$\bar{\sigma} = \frac{1}{\sqrt{2}} [(\sigma_z - \sigma_r)^2 + (\sigma_r - \sigma_\theta)^2 + (\sigma_z - \sigma_\theta)^2]^{1/2} \quad (5)$$

**Research Article**

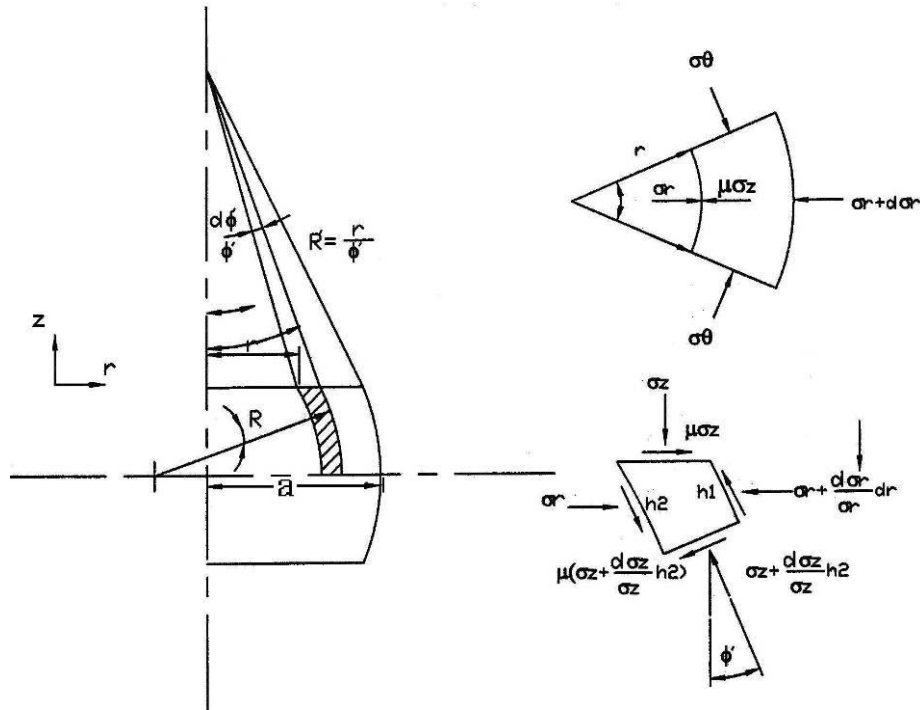


**Figure 2: Stress state and geometry of the element in the compression specimen between two flat and frictional frames (Milnick, 1981)**

In the above equations, the different parameters are as following:

$\sigma_\theta$ ,  $\sigma_z$  and  $\sigma_r$  the principal stresses in the peripheral and axial and radial directions respectively, and  $a$  is middle section radius of the specimen (Figure 2),  $r$  is the radius of the location of the desired element and  $R$  is the radius of curvature of the barrel lateral side of the sample. Compressive force  $P$  at each section of the sample is given by the following equation:

$$P = \int_0^a S_z 2\pi r dr = \pi a^2 (S_z)_{ave} \quad (6)$$

$$P = \pi \bar{\sigma} (2Ra - a^2) \ln\left(\frac{2R}{2R - a}\right) \quad (7)$$

Therefore, the material flow stress is:

$$\bar{\sigma} = \frac{P}{\pi(2Ra - a^2) \ln\left(\frac{2R}{2R - a}\right)} \quad (8)$$

And the relationship between flow stress ( $\bar{\sigma}$ ) and axial average stress, i.e.  $(\sigma_z)_{ave}$  is as following:

$$\bar{\sigma} = (\sigma_z)_{ave} \left[ \left(1 - \frac{2R}{a}\right) \ln\left(1 - \frac{a}{2R}\right) \right]^{-1} \quad (9)$$

The following equation can be displayed as follows:

$$\bar{\sigma} = (\sigma_z)_{ave} \hat{C}, \quad \hat{C} = \left[ \left(1 - \frac{2R}{a}\right) \ln\left(1 - \frac{a}{2R}\right) \right]^{-1} \quad (10)$$

Where,  $C'$  is called convexity correction factor. The value of  $R$  is the radius of curvature of the barreled sample as shown in Figure (3). This radius can be obtained based on the size of the different parts of the barreled sample. For this purpose, the following formula is used:

**Research Article**

$$R = \frac{h^2 + (d_2 - d_1)^2}{4(d_2 - d_1)} \quad (11)$$

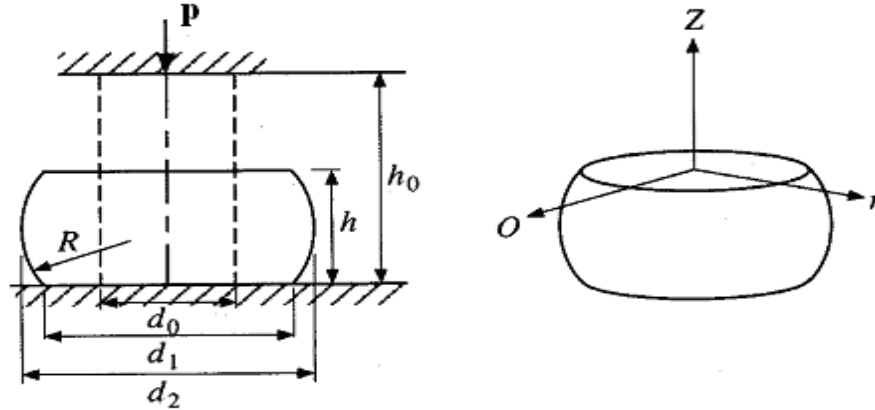


**Figure 3: The geometry of the barreled sample in the pressure test under the intra-surface friction (Milnick, 1981)**

*The Method of Numerical Correction Factor*

In high strains, convexity correction factor cannot correct well the effect of barreling of the specimen and flow stress. Therefore, the numerical correction coefficient is used to correct for better results (Saniei and Fatehi, 2006). The numerical correction coefficient with finite element simulation of pressure test using stress-strain curve obtained from convexity correction factor is performed in the first step of the simulation. Then by measuring the height of the sample in several stages, in order to calculate the equivalent strain and measure the diameter in the middle level of the simulated specimen such as pressure testing, by dividing the force resulted from simulation on the middle section of the specimen, the average strain is calculated. By dividing the obtained average stress on the stress-strain curve in each equivalent strain, the numbers obtained from this division are multiplied by the average stress-strain curve of the experiment. By re-simulation of the experiment using stress-strain curve obtained, the above steps are repeated. Usually by two or three repetitions of the simulation, the obtained stress-strain curve does not change and the final and accurate numerical correction coefficients are obtained (Saniei and Fatehi, 2006).

Many parameters influence the correction factor, including the friction coefficient, the ratio of height to diameter of the sample, hardening or softening strain of materials. In figure (4), the convexity correction factor and numerical correction factor have been drawn based on the ratio of  $R/a$ . In the case that the reduction in height is small, the strain is lower, and the ratio of  $R/a$  is larger and both methods have almost the same correction factor. But at high strains and when the ratio of  $R/a$  has considerably reduced, the completely different results are obtained for convexity correction factor and numerical correction factor. Convexity correction factor has continuously increased, but numerical correction coefficient reduces after a certain deformation. It can be argued that for high levels of strain, the effect of the output friction and shaping force are considerably increased. Therefore, to eliminate the enhanced effect of friction and determine material flow stress accurately, the correction factor value must be reduced (Saniei and Fatehi, 2006).

In figure (5), the changes of the numerical correction factor in different friction conditions is shown. It is well known that in low friction, the value of numerical correction factor is close to 1. However, for high friction, the fluctuation of correction coefficient is significant and in high strains the reduction value of correction factor in the elevated friction, is higher. In the first stage of pressure testing, the numerical correction factor is increased, since in the middle plate of the specimen, there is a free flow of materials

**Research Article**

and the shaping force is distributed on a completely large region, that is, the maximum area which is the same middle section. Therefore, the obtained stress is smaller than material flow, and it should be multiplied by a coefficient larger than 1. But with the advance of the process, the numerical correction factor decreases. This decrease is due to an increase in the effect of friction in the forming force.

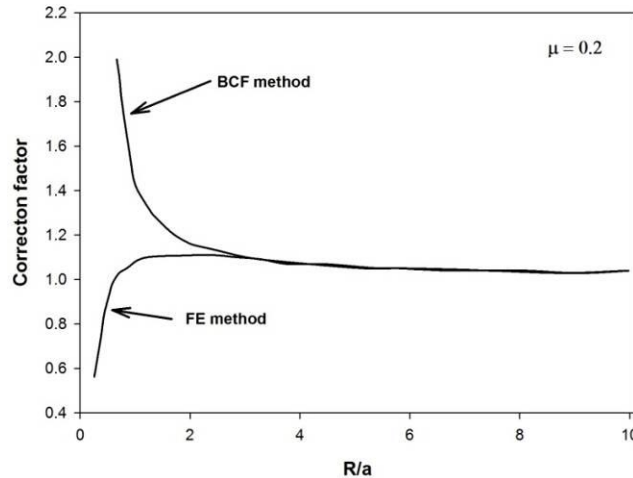


**Figure 4: The changes of convexity correction factor and numerical correction factor in terms of the ratio of  $R/a$**

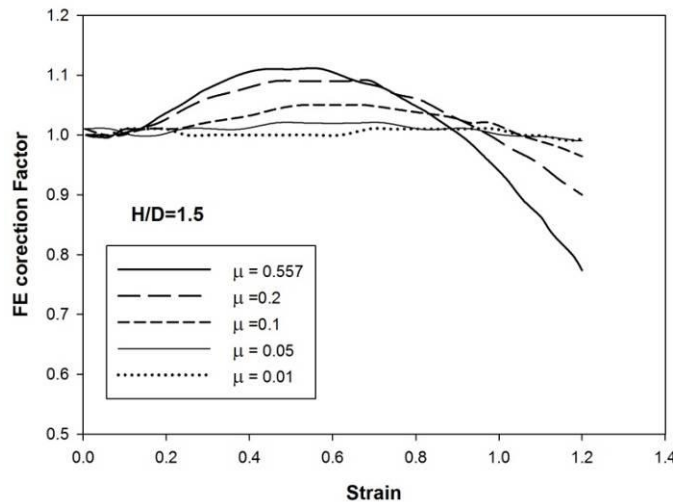


**Figure 5: The effect of friction factor on the numerical correction factor (Saniei and Fatehi, 2006)**

**Description Pressure Test**

Pressure test has been used to determine the flow curve of AZ60 alloy. In performing the tests carried out, the following points have been considered:

1. In each experiment, the sample has been kept for five minutes at the desired temperature.
2. The experiments were performed without lubrication.
3. The dimensional ratio of the sample has been based on the ASTM standard (height to diameter ratio equal to 1.5).
4. The strain rate at the pressure test has been kept constant.

**The Specification of the Specimen**

All samples have a diameter of 6mm and height of 9mm. Samples were prepared by machining. To remove any surface defects and possible stress concentration, the turned surfaces were smoothed using

**Research Article**

sandpaper with different degrees of harness. The experiments were performed by 150kNSANTAM apparatus which is shown in Figure (6). The experiment device is equipped with two fixed and movable jaws. The speed of the upper jaw is adjustable. To perform pressure test, at least 5 identical cylindrical specimens were turned for each curve and then to ensure the homogeneity of the samples, each specimen was separately pressed.



**Figure 6: SANTAM 150KN test apparatus used in the experiments**

**RESULTS AND DISCUSSION**

**Results and Analyses**

*Results of AZ60 Alloy Pressure Tests*

The pressure tests of AZ60 alloy magnesium were done on the samples at room temperature and under the compressor velocity of 0.5-5 mm/min. The obtained results are summarized in tables 1 to 4.

**Table 1: The results of pressure test for AZ60 alloy at room temperature and a constant speed of 5mm/min**

No.	Force (N)	Final height (mm)	Final Mid Radius (mm)	BCF
1	3583.25	8.92	3.011	1.0011
2	4359.78	8.85	3.018	1.0024
3	5214.83	8.61	3.08	1.0025
4	5777.54	8.43	3.04	1.0029
5	6466.64	8.22	3.06	1.0032
6	7519.18	8.11	3.12	1.0039
7	8798.21	7.91	3.17	1.0041
8	11719.26	7.89	3.21	1.0043

**Research Article**

**Table 2: The results of pressure test for AZ60 alloy at room temperature and a constant speed of 2mm/min**

No.	Force (N)	Final height (mm)	Final Mid Radius (mm)	BCF
1	3553.00	8.89	3.01	1.0011
2	4299.78	8.75	3.08	1.0024
3	5114.83	8.61	3.18	1.0025
4	5717.54	8.43	3.04	1.0029
5	6266.64	8.22	3.06	1.0032
6	7319.18	8.11	3.12	1.0039
7	8498.21	8.03	3.17	1.0041
8	11119.26	7.79	3.21	1.0043

**Table 3: The results of pressure test for AZ60 alloy at room temperature and a constant speed of 1mm/min**

No.	Force (N)	Final height (mm)	Final Mid Radius (mm)	BCF
1	3534.43	8.89	3.009	1.0009
2	4259.4	8.73	3.014	1.0018
3	5018.83	8.67	3.017	1.0021
4	5667.58	8.43	3.04	1.0029
5	6166.75	8.22	3.06	1.0032
6	7219.79	8.11	3.12	1.0039
7	8398.54	8.03	3.17	1.0041
8	10986.26	7.79	3.21	1.0043

**Table 4: The results of pressure test for AZ60 alloy at room temperature and a constant speed of 0.5mm/min**

No.	Force (N)	Final height (mm)	Final Mid Radius (mm)	BCF
1	3532.4	8.90	3.009	1.0009
2	4239.4	8.73	3.013	1.0018
3	5000.6	8.67	3.016	1.0021
4	5608.5	8.43	3.032	1.0029
5	6066.2	8.22	3.053	1.0032
6	7189.4	8.11	3.124	1.0038
7	8308.9	8.03	3.168	1.0040
8	10886.4	7.79	3.201	1.0041

In obtaining the stress and strain results in tables above, the following relations have been used:

**Research Article**

$$\varepsilon = \ln \frac{\text{Final Height}}{9} \tag{12}$$

$$\sigma = \frac{F}{\pi r^2} \times BCF \tag{13}$$

Initial values of stress have been summarized in tables 5 to 8 considering the convexity correction factor.

**Table 5: The stress-strain results of compression test at room temperature and speed of 5 mm/min**

	0.0089	0.017	0.045	0.066	0.091	0.105	0.0133	0.014
$\sigma$ (Mpa)	126.012	152.804	175.506	199.675	220.664	246.957	279.977	363.767

**Table 6: The stress-strain results of compression test for AZ60alloy at room temperature and speed of 2mm/min**

	0.0123	0.0282	0.0444	0.0655	0.091	0.105	0.863	0.145
$\sigma$ (Mpa)	125.028	144.695	161.484	197.601	213.82	240.388	270.43	345.143

**Table 7: The stress-strain results of compression test for AZ60alloy at room temperature and speed of 1mm/min**

	0.0123	0.0305	0.0374	0.0655	0.0907	0.105	0.115	0.145
$\sigma$ (Mpa)	124.433	149.593	175.967	195.874	210.412	237.124	267.259	341.015

**Table 8: The stress-strain results of compression test for AZ60alloy at room temperature and speed of 0.5mm/min**

	0.0112	0.0305	0.0374	0.0655	0.0907	0.105	0.115	0.145
$\sigma$ (Mpa)	124.361	148.990	175.444	194.857	207.931	235.498	264.714	339.750

Based on the results of tables 5 to 8, the stress-strain form of AZ60 alloy at room temperature is plotted in Figure 7.

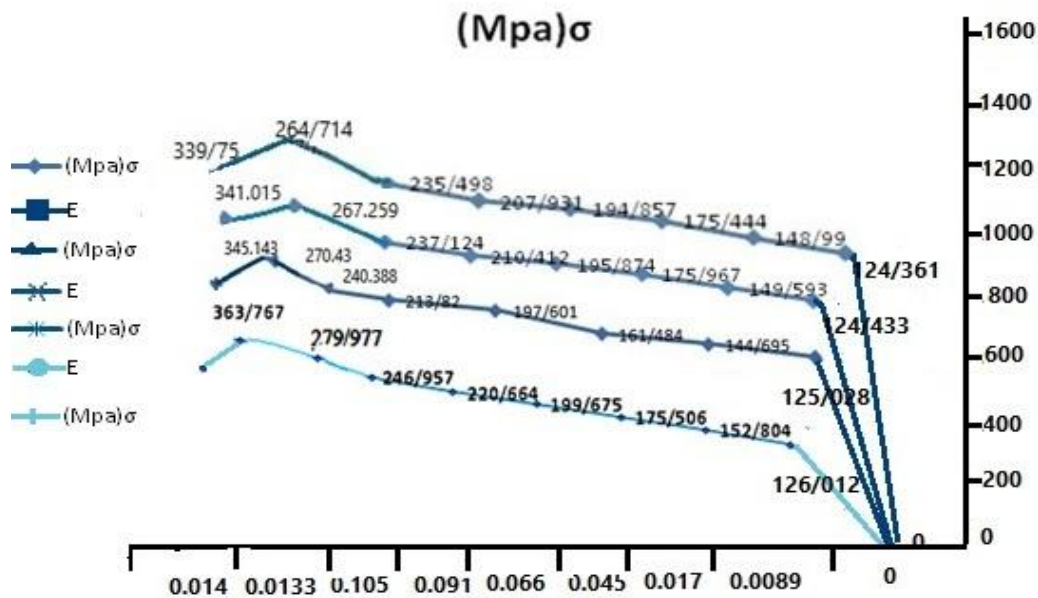


**Figure 7: The results of the stress-strain for AZ60 alloy at room temperature for different speeds**

## Research Article

### Numerical Correction Factor Method

Deform software is a finite element method that has been designed for simulation and analysis of the various processes of shaping and hot treatments. According to table to compare the obtained results from experiments and by convexity correction method, the results obtained from numerical correction method do not show significant differences. The curves of strain-stress of AZ60 alloy have been extracted based on the obtained results, and since the strains are low at room temperature, at low strains the stress values calculated from numerical correction factor and convexity correction factor have negligible differences; therefore, convexity correction factor method is an appropriate method for this alloy at room temperature. As can be seen in the tables above, this magnesium alloy has hardness behavior. With increasing strain, the stress rapidly increases to reach the point of failure.

### Conclusion

In this paper, compressive flow stress curves of AZ60 magnesium alloy was obtained. In this work, compression experiments were done on cylindrical specimens of AZ60 magnesium alloy at room temperature with different speeds between 0.5 to 5mm/min. The experiments were carried out by a device called SANTAM 150KN. Initial value of stress was calculated from convexity correction factor, and then by Deform-2D software and multi-stage correction, numerical values of stress-strain were obtained for the alloy. The results are as following:

1. First, with increasing strain, the stress is rapidly increased to the maximum point and in fact, the material has the hardening behavior.
2. At room temperature, with increasing the loading rate of compressor, stress-strain curve does not change much.
3. The convexity correction factor is fully geometric and the effect of other parameters affecting the deformation process is not considered.
4. In stress-strain curves of AZ60 alloy, at room temperature, stress values calculated from simulation software and convexity correction factor are slightly different.

## REFERENCES

- Anbuselvan S and Ramanathan S (2010).** Hot Deformation and processing maps of extruded magnesium Alloy Ze41A. *Materials & Design* **31**(2) 319-2, 323.
- Barati F, Fereshteh-Saniee F, Badnava H and Fallah Nejad K (2012).** An exponential model for prediction of the material flow curves of magnesium alloys in tension and compression several AZ series. *Materials and Design* **35** 1-11.
- Chang L, Wang Y, Zhao X and Huang J (2008).** Microstructure and mechanical properties in Az31 magnesium Alloy Fabricated by Asymmetric hot extrusion sheet. *Materials Science and Engineering A* **496** 512-516.
- Changizian P, Zarei-Hanzaki A and Roostaei A (2012).** The high temperature flow behavior modeling of Az81 magnesium Alloy Considering strain effects. *Materials and Design* **39** 384-389.
- Chen Q, Lin J, Shu D, Hu C, Zhao Z and Kang F (2012).** Development Microstructure, mechanical properties and formability of Mg-Zn-Y-Zr Alloy magnesium. *Materials Science and Engineering A* **554** 129-141.
- Chen X, Pan F, Mao J, Wang J, Zhang D and Tang A (2011).** Effect of heat treatment on strain hardening of Mg Alloy Zk60. *Materials and Design* **32** 1526-1530.
- Fereshteh-Saniee F and Fatehi-Sichani F (2006).** An investigation on determination of flow curves at Roomtemperature and under forming conditions. *Journal of Materials Processing Technology* **177** 478-482.
- Fu-sheng P, Jian-jun M, Xian-hua C, Jian P and Jing-feng W (2010).** Influence of Impurities on Microstructure and mechanical properties of magnesium Alloy Zk60. *Transactions of Nonferrous Metals Society of China* 1299-1, 304.
- He X, Yu Z, Liu G, Wang W and Lai X (2009).** Mathematical modeling for high temperature flow behavior of Ti-45Al-8.5Nb- as-cast (W, B, Y) Alloy. *Materials and Design* **30** 166-169.

### **Research Article**

**He Y, Pan Q, Qin Y, Liu X, Li W and Chiu Y et al., (2010).** Microstructure and mechanical properties of Zk60 Alloy Processed by equal channel angular Pressing two-step. *Journal of Alloys and Compounds* **492** 605-610.

**Kim WJ, Lee MJ, Lee BH and Park YB (2010).** A strategy for creating ultrafine-grained magnesium Alloy Microstructure in sheets. *Materials Letters* **64** 647-649.

**Legerski M, Schindler I, Kubina T and Hadasik E (2011).** Model of static re-crystallization of magnesium alloy AZ31.

**Li C and Dong Yu Y (2013).** The effect of solution heat Treatments on the Microstructure and hardness of magnesium alloys prepared Zk60-frequency alternating magnetic fields under low. *Materials Science & Engineering A* **559** 22-28.

**Li H, Wang H, Li Z, Liu C and Liu H (2010).** Flow behavior of as-cast Mg-10Gd and processing map-4.8Y-2Zn-0.6Zr Alloy. *Materials Science and Engineering A* **528** 154-160.

**Maksoud IA, Ahmed H and Rödel J (2009).** Investigation of the effect of strain rate and temperature on the Deformability and magnesium Alloy Microstructure evolution of Az31. *Materials Science and Engineering A* **504** 40-48.

**Mielnik EM (1991).** *Metalworking Science and Engineering* (McGraw Hill International Book Company).

**Polmear IJ (1981).** *Light Alloys* (Butterworth-Heinemann).

**Qin YJ, Pan QL, He YB, Li WB, Liu XY and Fan X (2010).** Modeling of flow stress during hot Deformation for magnesium Alloy. *Materials Science and Engineering A* **527** 2790-2797.

**Renlong X, Bingshu W, Xinpin C and Quin Liu (2009).** Examination of dynamic Re-crystallization Az31 during compression of magnesium. *Science in China Series E: Technological Sciences* **52** 176-179.

**Sheng Z and Shivpuri R (2006).** Flow stress of magnesium alloys at elevated temperature modeling. *Materials Science and Engineering A* **419** 202-208.

**Song WQ, Beggs P and Easton M (2009).** Compressive strain-rate sensitivity of magnesium-aluminum die casting alloys. *Materials & Design* **30** 642-648.

**Wang C, Wang X, Chang H, Wu K and Zheng M (2007).** Processing maps for hot working of magnesium Alloy Zk60. *Materials Science and Engineering* **464** 52-58.

**Wu YZ, Yan HG, Chen JH, Zhu SQ, Su B and Zeng PL (2010).** Hot Deformation Microstructure evolution and behavior of magnesium Alloy Zk21. *Materials Science and Engineering A* **527**(3) 670-3, 675.

**Xin W, Wen-zhen C, Lian-xi H, Guo-jun W and Er-de W (2011).** Refining Microstructure and property improvement of magnesium Alloy Zk60 by hot rolling. *Transactions of Nonferrous Metals Society of China* 226-242.

**Yan L, Zhi-min Z and Yong X (2011).** Influence of aging on Microstructure and mechanical properties of magnesium alloys Az80 and Zk60. *Transactions of Nonferrous Metals Society of China* **21** 739-744.

**Yang Y, Li B and Zhang Z (2009).** Flow stress of wrought magnesium alloys during hot compression at medium and high Temperatures Deformation. *Materials Science and Engineering A* **499** 238-241.

**Ya-qin Y, Bao-cheng L and Zhi-min Z (2008).** Deformation analysis on flow stress of magnesium alloys during high temperature. *Transactions of Nonferrous Metals Society of China* **18** 180-184.

**Ying-liang C, Ting-wei Q, Hui-min W and Zhao Z (2009).** Comparison of corrosion behaviors of Az31, Az91, Am60 and Zk60 magnesium alloys. *Transactions of Nonferrous Metals Society of China* **19** 517-524.

**Yong L (2008).** Deformation behavior of Ti-6Al compressive Hot and Microstructure evolution 2Zr-1Mo-1V-Alloy at 1073K. *Materials Science and Engineering A* **490** 113-116.

**Yun-bin H, Qing-lin P, Qin C, Zhi-ye Z, Xiao-yan L and Wen-bin L (2012).** A dynamic modeling of strain hardening during hot Deformation Recrystallization of Zk60 magnesium Alloy. *Transactions of Nonferrous Metals Society of China* **22** 246-254.